Friction **1**(1): 81–91 (2013)
DOI 10.1007/s40544-013-0007-1 ISSN 2223-7690
RESEARCH ARTICLE

Running-in process of Si–SiO_x/SiO_2 pair at nanoscale—Sharp drops in friction and wear rate during initial cycles

Lei CHEN[1], **Seong H. KIM**[2], **Xiaodong WANG**[1], **Linmao QIAN**[1,*]

[1] *Tribology Research Institute, National Traction Power Laboratory, Southwest Jiaotong University, Chengdu 610031, China*

[2] *Department of Chemical Engineering, The Pennsylvania State University, University Park, Pennsylvania 16802, USA*

Received: 13 November 2012 / Revised: 25 January 2013 / Accepted: 21 February 2013

Abstract: Using an atomic force microscope, the running-in process of a single crystalline silicon wafer coated with native oxide layer (Si–SiO_x) against a SiO_2 microsphere was investigated under various normal loads and displacement amplitudes in ambient air. As the number of sliding cycles increased, both the friction force F_t of the Si–SiO_x/SiO_2 pair and the wear rate of the silicon surface showed sharp drops during the initial 50 cycles and then leveled off in the remaining cycles. The sharp drop in F_t appeared to be induced mainly by the reduction of adhesion-related interfacial force between the Si–SiO_x/SiO_2 pair. During the running-in process, the contact area of the Si–SiO_x/SiO_2 pair might become hydrophobic due to removal of the hydrophilic oxide layer on the silicon surface and the surface change of the SiO_2 tip, which caused the reduction of friction force and the wear rate of the Si–SiO_x/SiO_2 pair. A phenomenological model is proposed to explain the running-in process of the Si–SiO_x/SiO_2 pair in ambient air. The results may help us understand the mechanism of the running-in process of the Si–SiO_x/SiO_2 pair at nanoscale and reduce wear failure in dynamic microelectromechanical systems (MEMS).

Keywords: nanotribology; friction; nanowear; running-in process; silicon; atomic force microscope

1 Introduction

With the development of lithographic microfabrication and micromachining techniques, silicon has become a principal construction material in microelectromechanical systems (MEMS) [1, 2]. When the dimensions shrink to nanoscale, the ratio of surface area to volume greatly increases so that the interfacial forces become dominant [3]. As a result, the nanotribological problems involving friction, adhesion, and wear, have become an important concern in Si-MEMS [2–4].

As a well-known tribological process, running-in is usually defined as the initial operation of a friction pair until certain friction force and wear rate have reached a steady state [5]. In macroscale devices, surface roughness, apparent defects, and surface waviness induced by manufacturing can affect running-in behavior [6–8]. Many new machine parts, such as cylinders and gears, often need to be conditioned through running-in before they are placed into regular service. During running-in, because the peaks of asperities on rough contact surfaces are removed by mechanical interactions and valleys are filled by wear debris, the average surface roughness of specimens would decrease to a stable state [7, 8]. The generation of wear debris as a three-body layer might lubricate contact interfaces [9, 10]. As a result, both the friction force and the wear rate may decrease and then level off during macroscale running-in.

However, when tests are performed at nanoscale, counter pair normally contact with a single asperity mode due to nanoscale roughness and nanoscale contact area. In this case, the traditional running-in mechanism may not be valid during nanowear process. Nevertheless, similar to running-in processes in macroscale devices, running-in processes in nanoscale

* Corresponding author: Linmao QIAN.
E-mail: linmao@swjtu.edu.cn

devices are often observed [11]. Therefore, it is essential to understand the running-in process in the friction pair of nanoscale devices and the variation of the friction force and wear during initial sliding cycles.

In this study, the running-in process of single crystalline silicon coated with native oxide (Si–SiO_x) against a SiO_2 microsphere was investigated using an atomic force microscope in ambient air. The mechanism is discussed based on an analysis of the friction-induced reduction of adhesion of the Si–SiO_x/SiO_2 pair. Finally, a phenomenological model based on the results for friction and nanowear is proposed to explain the running-in process of the Si–SiO_x/SiO_2 pair in ambient air.

2 Material and methods

Wafers of p-Si(100) with thicknesses of 0.5 mm were purchased from MEMC Electronic Materials, Inc., USA. The root-mean-square (RMS) roughness of each silicon wafer was about 0.07 nm over a 500 × 500 nm area. To simulate the real surfaces of dynamic MEMS, the native oxide layers on the silicon surfaces were not removed. Each surface was partially covered with Si–OH groups, which showed relatively hydrophilic with a water contact angle of 39°. Hereafter, this substrate will be called "Si–SiO_x". As a comparison, a hydrophobic silicon sample was obtained by immersing the original silicon in a 40% aqueous solution of hydrofluoric acid for 2 min, followed by rinsing in distilled water and methanol [12]. Due to the termination of Si–H groups on the silicon surface, this sample was relatively hydrophobic with a water contact angle of 83°. Hereafter, "Si–H" is used to denote this hydrophobic silicon sample.

Nanowear tests of native oxide-coated silicon wafers against SiO_2 tips (Si–SiO_x/SiO_2 pair) were performed with an atomic force microscope (AFM, SPI3800N, Seiko, Japan) in an environment chamber with a vacuum capability. As shown in Fig. 1, the SiO_2 tip with a radius of 1 μm (Novascan Technologies, USA) moved horizontally on the silicon wafer surface under a normal load F_n. The inset pictures show SEM images of the SiO_2 microsphere and its cantilever. Using a calibration probe with a force constant of 2.957 N/m,

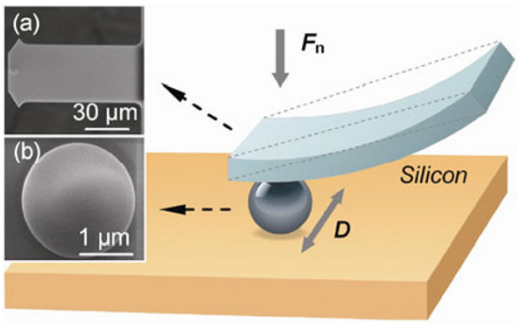

Fig. 1 The schematic illustration showing the nanowear test. The SiO_2 microspheric tip moved horizontally on the silicon surface with a displacement amplitude D under a normal load F_n. The inset pictures show the SEM images of the cantilever of AFM probe (a) and the SiO_2 microsphere (b).

the normal spring constants of the cantilever of SiO_2 tips were calibrated to be 10.5–13.8 N/m [13]. If not specially mentioned, the applied normal load F_n was 5 μN, the sliding speed was 0.8 μm/s, the number of sliding cycles was 2000, and the displacement amplitude D was 100 nm. The total sliding distance in each cycle was 4D. All tests were carried out in air with a relative humidity (RH) of 50%–60% and room temperature of 20 ˚C–25 ˚C. After tests, friction forces were calibrated using a silicon grating with a wedge angle of 54°44′ (TGF11, MikroMasch, Germany) [14]. To characterize the adhesive behavior of Si–SiO_x/SiO_2 pair, the average adhesion forces F_a were obtained by twenty pull-off tests. After nanowear tests, the topography of the wear area was scanned by a sensitive silicon nitride tip (MLCT, Veeco, USA), which had a curvature radius of 20 nm and a nominal spring constant of 0.1 N/m.

3 Results

3.1 Running-in process of Si/SiO_2 pair

The friction loops and forces for the Si–SiO_x/SiO_2 pair are plotted as a function of the number of sliding cycles N in Fig. 2. The friction loops presented four different shapes over various numbers of sliding cycles, as shown in the inset pictures of Fig. 2. During the first several cycles, the friction loop was in a parallelogram shape, which has been observed elsewhere [15, 16]. At the fifth cycle, the parallelogram quickly changed to the shape of an hourglass. After 50 cycles,

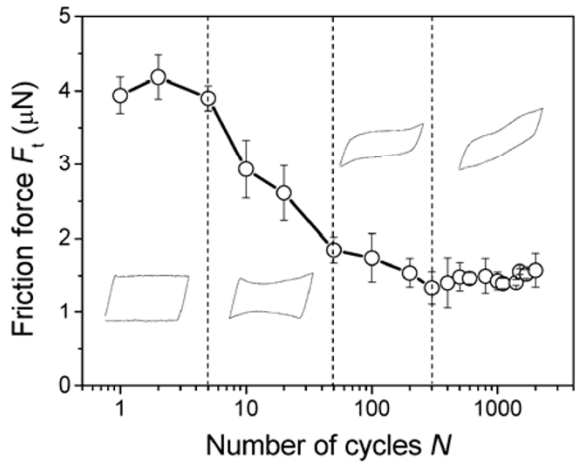

Fig. 2 The friction force F_t versus the number of sliding cycles N (F_t–N) curves of Si–SiO_x/SiO_2 pair in air. The inset pictures show the variation of the shape of tangential force F versus displacement d (F~δ) curves with N. The normal load F_n = 5 μN, displacement amplitude D = 100 nm.

an ellipse shape with force peaks appeared. When the number of sliding cycles increased to about 200, the friction loops finally changed to an oblique parallelogram, which was preserved throughout the remaining cycles.

Because the shape of the friction loop changed as N increased, the friction force F_t could not be calculated by simply taking the force difference between the forward and backward directions and dividing by two. Instead, the average F_t was calculated by dividing the total energy dissipated in a sliding cycle (E) by the total sliding distance per cycle ($4D$) [17]:

$$F_t = \frac{E}{4D} \tag{1}$$

In the first cycle, the friction force F_t of the Si–SiO_x/SiO_2 pair was 3.9 μN. As the number of sliding cycles N increased, F_t exhibited a sharp decrease during the first 50 cycles, gradually decreased between 50 and 300 cycles, and then maintained a stable value in the remaining cycles up to N = 2000. Compared to F_t in the first cycle, the stable value of the friction force decreased by about 62% after the running-in process.

The change in shape of the friction loops shown in Fig. 2 is related to the wear of the silicon surface [18]. After the nanowear tests, the resulting wear scars were scanned with a sharp Si_3N_4 tip, as shown in Fig. 3(a). Although the contact pressure (1.3 GPa) between the SiO_2 tip and the silicon surface under a normal load of 5 μN was far less than the yield limit of monocrystalline silicon (7 GPa), material loss occurred and, after only five sliding cycles, a groove with a depth of 1.3 nm was created on the silicon surface [19]. As the number of sliding cycles increased, wear on the silicon surface became more severe, and the wear depth increased to 55 nm after 2000 cycles. To quantitatively characterize the wear behavior of the silicon surface during the running-in process, the wear rate γ was calculated by

$$\gamma = \frac{\phi}{(F_n + F_a)l} \tag{2}$$

where Φ is the wear volume and l is the total sliding distance (= $4D \times N$). As shown in Fig. 3(b), the wear rate γ of the silicon surface underwent a sharp drop during the initial 50 sliding cycles, then gradually decreased to a constant value over the remaining cycles.

3.2 Effect of load and displacement amplitude on the running-in process of Si–SiO_x/SiO_2 pair

To investigate the effects of experimental conditions on the running-in process, tests were performed at various normal loads F_n and displacement amplitudes D in humid air. Figure 4(a) shows F_t–N curves of the Si–SiO_x/SiO_2 pair obtained at normal loads of 0.5 μN, 3 μN, and 5 μN. The inset picture shows the friction coefficient μ as a function of sliding cycles under the three loads. Here, μ was determined by $\mu = F_t/L$, where L is the sum of the normal load F_n and the adhesion force F_a between tip and silicon sample. As the number of sliding cycles increased, both the friction force F_t and the friction coefficient μ, at all tested loads, exhibited a sharp drop within the initial 50 cycles, then gradually decreased to stable values during the remaining cycles. Compared to the initial friction force, the stable friction force was reduced by 74%, 69%, and 62% at normal loads of 0.5 μN, 3 μN, and 5 μN, respectively. When the normal load was lower, the degree of friction reduction was larger. Figure 4(b) shows wear scars on the silicon surface after 2000 cycles. Grooves having depths of 19 nm, 40 nm, and 55 nm were generated on the silicon surface under applied normal loads of 0.5 μN, 3 μN, and 5 μN, respectively.

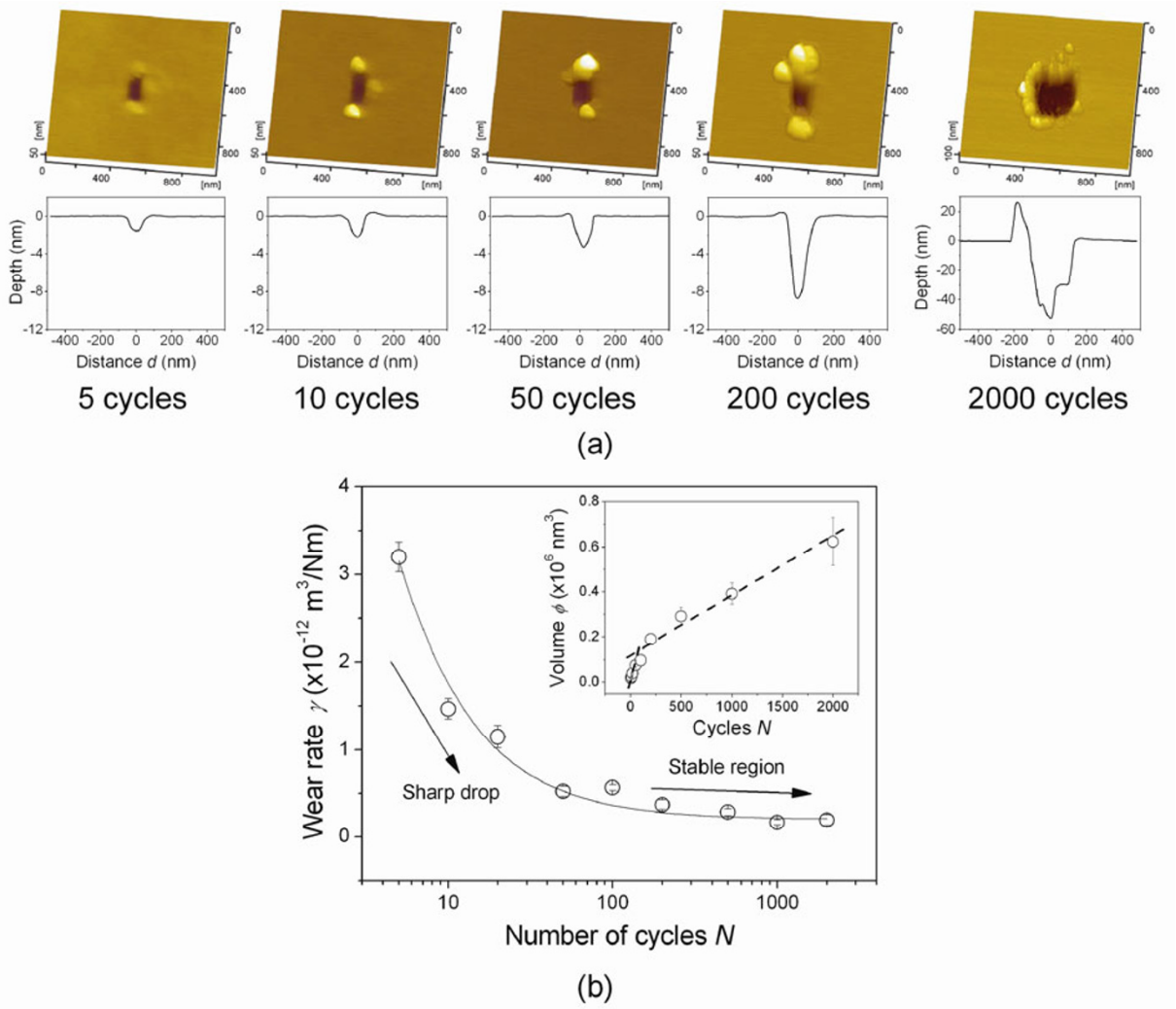

Fig. 3 (a) The AFM images and cross-section profiles of scars on silicon surface after various cycles of wear tests. (b) The wear rate γ of silicon surface plotted as the function of sliding cycle. The inset shows the variation of wear volume Φ with the increase of sliding cycles.

However, the friction loops at 2000 cycles presented different behaviors under the three displacement amplitudes D tested, as shown in Fig. 5(b). When D = 100 nm or 250 nm, the vertical section of the wear scars showed a camber shape and the friction loops formed an oblique parallelogram at 2000 cycles. But when D = 500 nm, the vertical section of the wear scars was in a U slot shape. Since the wear scar had enough space for SiO_2 tip sliding, the friction force exhibited stable values within the central 400 nm and revealed peaked forces at the edges of the wear scars. These results indicate that the shape of the friction loop of Si–SiO_x/SiO_2 pair was strongly dependent on the topography of wear scars on the silicon surface [18].

Figure 5(a) exhibits F_t–N curves of the Si–SiO_x/SiO_2 pair at displacement amplitudes D of 100, 250, and 500 nm. Similar to that at D = 100 nm and F_n = 5 μN, the friction force decreased by about 62% during running-in processes at D = 250 and 500 nm. After 2000 cycles, grooves with depths of about 55 nm were formed regardless of the displacement amplitude, as shown in Fig. 5(b). Clearly, the influence of D (> 100 nm) on the friction behavior of the Si–SiO_x/SiO_2 pair and on wear of the silicon surface was negligible.

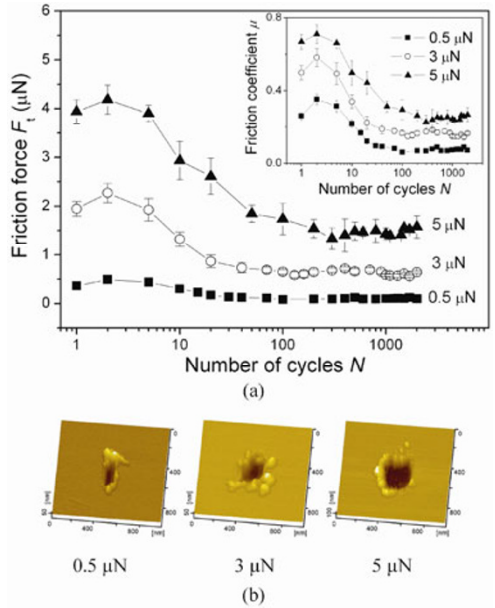

Fig. 4 (a) The F_t–N curves of Si–SiO_x/SiO_2 pair at various applied loads F_n. (b) The corresponding AFM images of scars on silicon surface under D = 100 nm and N = 2000. The inset picture in Fig. 4(a) shows the friction coefficient μ as the function of sliding cycles at various loads.

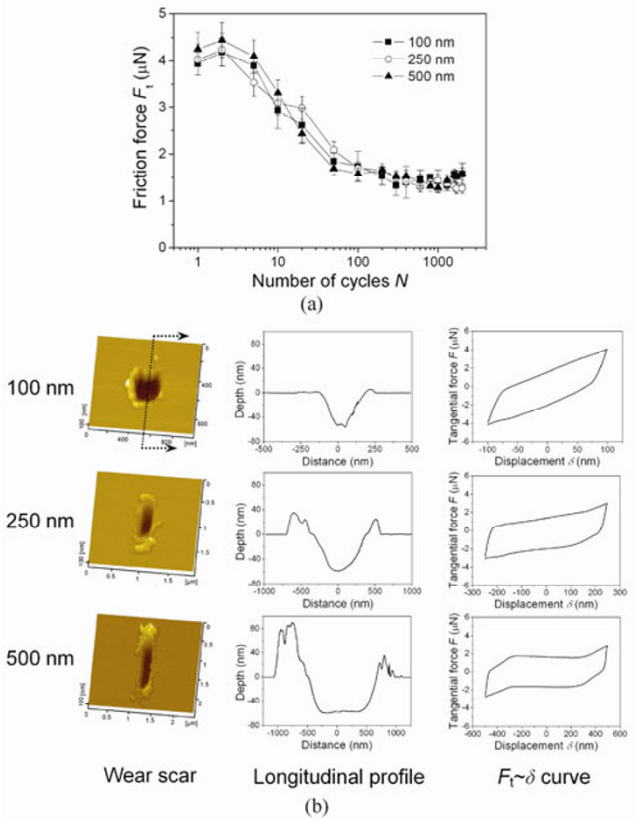

Fig. 5 (a) The F_t–N curves of Si–SiO_x/SiO_2 pair under various displacement amplitudes D. (b) Effect of the displacement amplitude on the shape of F~δ curves of Si–SiO_x/SiO_2 pair under F_n = 5 μN and N = 2000.

4 Discussion

4.1 Sharp drop of interfacial force during a running-in process

At macroscale, the decrease of friction during running-in process is normally attributed to the reduction in contact pressure after rough asperities on counter surfaces are flattened under mechanical action [7, 8]. In this experiment, since the SiO_2 microsphere and silicon surface provided a single asperity contact, the macroscale topographic smoothening mechanism cannot explain the sharp drop in friction force during the nanoscale running-in process of Si–SiO_x/SiO_2 pair.

At nanoscale, the traditional Amonton's law cannot be used to calculate the friction force. To analyze the running-in behavior of nanoscale friction, we adapt the model proposed by Tambe et al. [20], which assumes that the nanoscale friction force between contact interfaces is a result of three components: F_{int} due to interfacial adhesion, F_{def} due to deformation, and $F_{stick\text{-}slip}$ due to stick-slip of contact interfaces.

$$F_t = F_{int} + F_{def} + F_{stick\text{-}slip} \quad (3)$$

Since no jump of tip occurred in our tests, the contribution of $F_{stick\text{-}slip}$ can be neglected here, and the friction force F_t is mainly attributed to F_{def} and F_{int}. Although there could be some tribochemical contributions to wear, we assume that the substrate profile change in the wear track is mainly due to deformation.

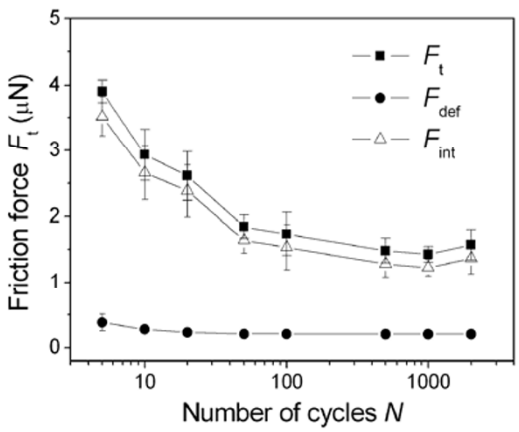

Fig. 6 Variation of the total friction force F_t, the deformation-related friction force F_{def} and the adhesion-related friction F_{adh} of Si–SiO_x/SiO_2 pair with the increase in sliding cycles.

This would, at least, give an upper limit to the deformation-related contribution to the friction. Due to the nonlinearity of the elastoplastic stress-strain relationship of silicon, it is difficult to precisely calculate the deformation component of the friction force F_{def}. Here, the deformation-related force F_{def} is estimated as the sum of the elastic deformation-related force $F_{def\text{-}e}$ and the plastic deformation-related force $F_{def\text{-}p}$. This may somewhat overestimate the value of F_{def}. $F_{def\text{-}e}$ can be determined by [21]

$$F_{def\text{-}e} = \frac{2L}{\pi a^2}(R^2 \sin^{-1}(a/R) - a\sqrt{R^2 - a^2}) \quad (4)$$

Here, R is the radius of the SiO_2 tip and a is the contact radius between tip and sample, which can be estimated by the DMT model. Using Eq. (4), $F_{def\text{-}e}$ was calculated to be 0.194 μN in the first sliding cycle under an adhesion force of 1.35 μN. When the number of sliding cycles increased to 2000, $F_{def\text{-}e}$ was estimated to be about 0.177 μN, considering the surface damage and the variation in the adhesion force (see Fig. 7). It seemed that $F_{def\text{-}e}$ changed only a little during the nanowear process.

If the loss of material on the silicon surface was fully attributed to mechanical interactions, $F_{def\text{-}p}$ could be estimated by [22]

$$F_{def\text{-}p} = S\sigma_y \quad (5)$$

where S is the projected area of plastic deformation along the sliding direction, and σ_y =7 GPa is the yield limit of monocrystalline silicon [19]. In each cycle, S could be estimated as

$$S = \frac{\Delta\phi}{2D} \quad (6)$$

where $\Delta\Phi$ is the wear volume on the silicon surface during each cycle. Using Eqs. (5) and (6), $F_{def\text{-}p}$ can be determined by

$$F_{def\text{-}p} = \frac{\Delta\phi\sigma_y}{2D} \quad (7)$$

Figure 6 shows the variation in F_{def} (= $F_{def\text{-}e}$ + $F_{def\text{-}p}$) and the rest of the friction component F_{int} (= $F_t - F_{def}$) of the Si–SiO_x/SiO_2 pair as the number of sliding cycles increases. Due to the existence of the oxide layer during the initial cycles and the formation of wear debris after several sliding cycles, the actual yield limit of the deformation area on the silicon substrate may be smaller than the yield limit of monocrystalline silicon cited above (7 GPa). As a result, the calculated values of F_{def} in Fig. 6 may be somewhat overestimated. However, F_{def} showed only a marginal decrease during the initial cycles and remained stable thereafter. These results indicate that substrate deformation cannot be the main cause for the sharp drop in friction force during the running-in process. Thus, the friction change during running-in can be mainly attributed to the reduction in the adhesion-related

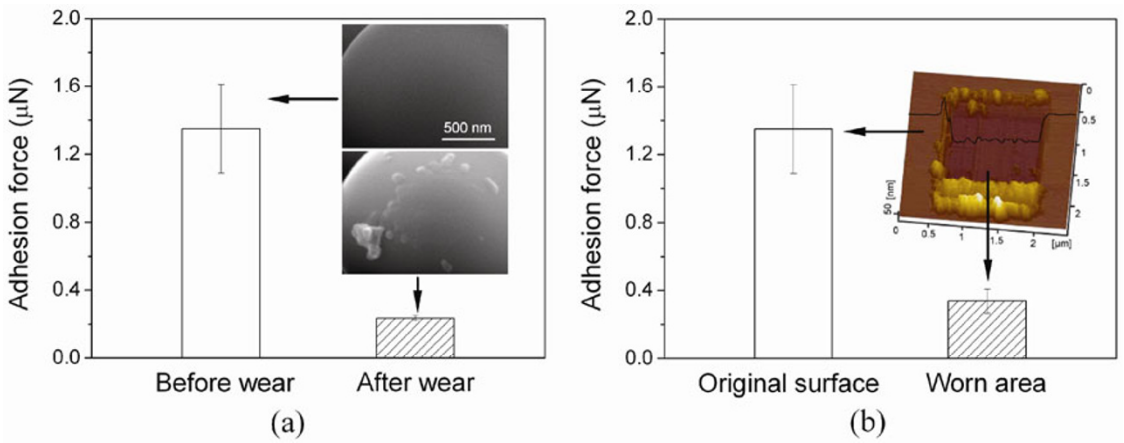

Fig. 7 (a) The adhesion force F_a of Si–SiO_x/SiO_2 pair measured on fresh silicon surface before and after wear test. The inset pictures show the SEM images of SiO_2 microsphere before and after wear test. (b) The adhesion force F_a measured on fresh silicon surface and on worn silicon surface by a new SiO_2 tip. The inset picture shows the AFM image and the corresponding vertical section of wear scar on Si–SiO_x surface.

interfacial force between the SiO_2 tip and the silicon surface.

4.2 Friction-induced reduction of adhesion during the running-in process

At nanoscale, variations in the interfacial force F_{int} are normally induced by the transformation of surface properties of the counter pair [23]. To detect changes in surface properties during running-in, the adhesion force F_a of the Si-SiO_x/SiO_2 pair was measured before and after wear tests.

Since the size of the wear scar was less than 200 nm × 300 nm under the given conditions, the SiO_2 tip was difficult to locate in the wear area during tests of the adhesion force F_a. As a result, F_a was measured on a fresh silicon surface by the SiO_2 tip before and after wear tests. As shown in Fig. 7(a), the value of F_a was 1.35 μN before the test and decreased to 0.24 μN (a reduction of ~82%) after 2000 sliding cycles. The inset pictures in Fig. 7(a) show SEM images of the SiO_2 tip before and after wear tests. The material transfer layer and wear debris can be observed on the contact area of the SiO_2 tip surface after wear tests. The deposition of substrate wear debris particles on the SiO_2 tip surface could reduce the actual contact area between the tip and substrate surface. This could contribute to the reduction in the adhesion force. Also, it is possible that the transferred silicon wear debris particles might make the tip surface more hydrophobic. If this happens, then the adhesion due to capillary effects could also be reduced [12, 24]. In any case, these changes in the tip surface topography and chemistry must be responsible for the overall reduction of the adhesion force of the SiO_2 tip after the wear test.

The thickness of the native oxide layer on a Si wafer is typically about 2 nm [25]. Since the wear depth during the initial running-in period is about 2–3 nm (Fig. 3(a)), it is reasonable to assume that the running-in process removes the hydrophilic silicon oxide layer. To verify this, a wear area having a depth of 5 nm was prepared on a silicon surface by scanning-scratch, as shown in the inset picture in Fig. 7(b). Using a new SiO_2 tip, F_a was detected on both fresh and worn silicon surfaces. As shown in Fig. 7(b), compared to that on the fresh silicon surface, F_a decreased by ~64% on the worn silicon surface. Based on IR spectra, Mizuhara and Hsu [26] indicated that oxygen is far less reactive than water. Thus, a new oxide layer has difficulty forming on a worn silicon surface during a sliding process. Therefore, the hydrophobic property of the worn silicon surface is attributed to removal of the hydrophilic oxide layer on the Si–SiO_x surface during running-in.

To further support this interpretation, the running-in process of a SiO_2 microsphere sliding against a Si–H surface was investigated. As shown in Fig. 8(a), unlike the Si–SiO_x/SiO_2 pair, no sharp drop in friction force was observed during the running-in process of the hydrophobic Si–H/SiO_2 pair. At a RH of 50%–60%, the thickness of the adsorbed water layer was estimated to be 0.98 nm on the native oxide-coated silicon surface and 0.4 nm on the hydrophobic Si–H surface [27]. Therefore, the initial friction behavior would have a large contribution from the capillarity effect on the native silicon oxide surface, which would be lacking on the Si–H surface [28]. As a result, the initial friction force of the Si–H/SiO_2 pair was much smaller than that of the Si–SiO_x/SiO_2 pair. However, when the native oxide layer was removed after 50 sliding cycles (Fig. 3(a)), the friction force of the Si–SiO_x/SiO_2 pair approached the value of the Si–H/SiO_2 pair (Fig. 8(a)).

Figures 8(b) and 8(c) show the wear scars after 2000 cycles on silicon and on Si–H surfaces, respectively. The wear rate of the Si–H/SiO_2 pair was ~0.26×10^{-12} m^3/Nm, which was very similar to the stable wear rate (~0.3×10^{-12} m^3/Nm) observed after the running-in period (~50 cycles) for the Si–SiO_x/SiO_2 pair. These results also suggest that the native oxide layer is removed

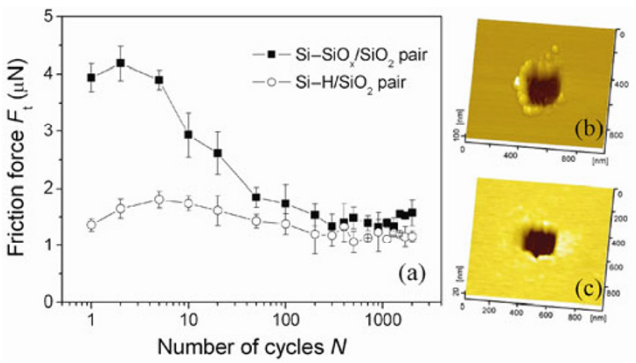

Fig. 8 The F_t–N curves of Si–SiO_x/SiO_2 pair and Si–H/SiO_2 pair (a) and the corresponding AFM images of scars on silicon surface (b) and on Si–H surface (c) under F_n = 5 μN, D = 100 nm, and N = 2000.

during the running-in process of the Si–SiO_x/SiO_2 pair. Such a running-in process has also been observed on macroscale silicon surfaces and DLC coating surfaces, where a sharp drop in friction force was attributed to the wear or removal of the surface oxide layer [10, 29].

Figure 9 compares the adhesion and friction forces before and after 2000 cycles of sliding for the Si–SiO_x/SiO_2 and Si–H/SiO_2 pairs. In the case of the Si–SiO_x/SiO_2 pair, the adhesion force decreased by ~75% and the friction force decreased by ~62% during running-in. For the Si–H/SiO_2 pair, the adhesion force and friction force decreased by only ~7% and ~9%, respectively. Clearly, the sharp drop in friction force corresponds to a sharp drop in adhesion force.

According to the results for the adhesion force (Fig. 7), both the surfaces of silicon substrate and the SiO_2 tip may change their behavior and induce a drop in friction force during running-in of the Si–SiO_x/SiO_2 pair. To detect how changes in the tip surface affect friction behavior, a new SiO_2 tip was first modified by repeated rubbing cycles on a clean substrate surface. After that, the friction force between the modified tip and the pre-worn silicon surface was measured in-situ. To have a comparison, the friction force between the modified tip and the original Si–SiO_x surface was measured at a new location. As shown in Fig. 10, the friction forces on both the worn and the original Si–SiO_x surfaces showed sharp drops as the number of sliding cycles increased. Further, all the friction forces measured on the worn silicon surface were a little lower than those measured on the original silicon surface. After 2000 sliding cycles, F_t decreased by about 50% on the original silicon and about 62% on the worn area. Therefore, modification of the SiO_2 tip during running-in also played some role in the sharp drop of friction force for the Si–SiO_x/SiO_2 pair.

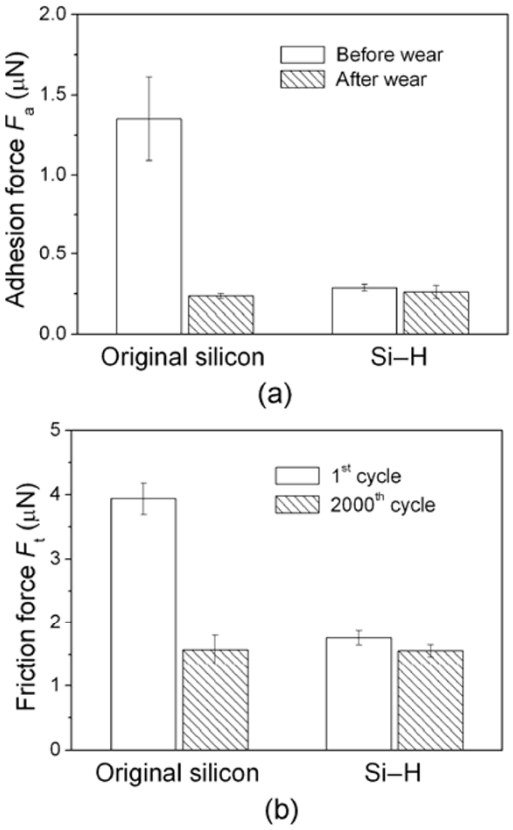

Fig. 9 (a) The adhesion force before and after wear tests of Si–SiO_x/SiO_2 pair and Si–H/SiO_2 pair. (b) The friction force in the 1st cycle and the 2000th cycle of Si–SiO_x/SiO_2 pair and Si–H/SiO_2 pair.

4.3 Mechanism of the running-in process of Si/SiO_2 pair

Figure 11 schematically shows the running-in process of the Si–SiO_x surface against a SiO_2 microsphere in ambient air. The silicon surface with a native oxide layer was partially covered with Si–OH groups, which allowed adsorption of water molecules from the humid air [12, 24]. While the tip slides on the silicon surface, a water bridge will form between the Si–SiO_x substrate and the SiO_2 tip surface, as shown in Fig. 11(a). As a result, both the friction force F_t and the wear rate exhibited a large value over the initial several cycles.

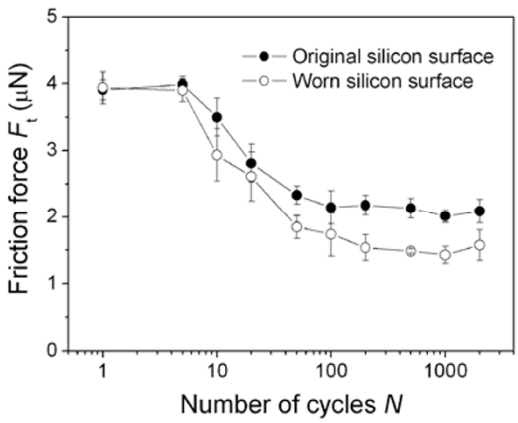

Fig. 10 The friction forces F_t measured on original and worn silicon surfaces by a new SiO_2 tip modified by certain numbers of sliding cycles.

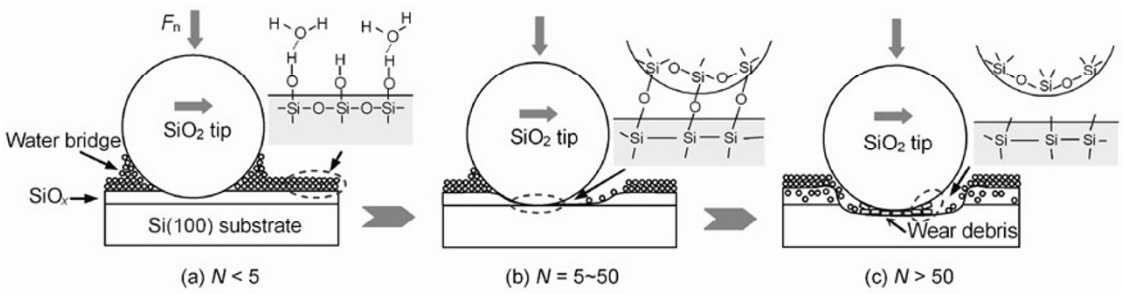

Fig. 11 The schematics showing the running-in process of Si–SiO_x/SiO_2 pair in humidity air. (a) $N < 5$, (b) $N = 5$~50, (c) $N > 50$.

However, when the native oxide layer on the Si–SiO_x surface was removed by the SiO_2 tip via water-induced corrosion [30, 31], the Si–Si network of the Si(100) substrate will be exposed to air, and the silicon surface becomes more hydrophobic due to the reduction of Si–OH groups [32]. Because of the reciprocating scratch by the SiO_2 tip, the Si–Si network could be broken by shear stresses transmitted from the Si–O–Si bridges between the SiO_2 tip and the silicon substrate, as shown in Fig. 11(b) [26, 33]. At the same time, the tip surface could become more hydrophobic because of dehydroxylation reactions during this process [12, 24]. Since the transformation of silanol bonds to siloxane bonds is exothermic, dehydroxylation reactions probably occur on the SiO_2 tip surface under shear stress during the initial sliding process [34]. The hydrophobization of the contact area on the SiO_2 tip and the silicon surface would reduce both the friction force and the wear rate, as shown in Fig. 11(c) [35, 36].

In summary, the sharp drops in friction force and wear rate during running-in were caused by hydrophobization of the SiO_2 tip and the silicon surface, as well as by lubrication provided by wear debris. Unlike mechanical interactions in macroscale devices, tribochemical reactions play a dominant role during running-in of nanoscale Si–SiO_x/SiO_2 pair.

5 Conclusions

Using an AFM, the running-in process of Si–SiO_x/SiO_2 pair in ambient air was investigated under various normal loads and displacement amplitudes. The main conclusions can be summarized as follows.

Nanowear of Si–SiO_x/SiO_2 pair exhibited a typical running-in process. During the initial 50 sliding cycles, the friction force of the Si–SiO_x/SiO_2 pair rapidly decreased to 40% of its initial value, and the wear rate on the silicon surface sharply decreased to 10% of its initial value. In the remaining sliding cycles up to 2000, both the friction force and the wear rate gradually decreased to constant values.

During running-in, the sharp drop in friction force between the silicon surface and the SiO_2 tip was mainly attributed to wear of the surface oxide layer and to change in the surface of the SiO_2 tip, which reduced adhesion-related interfacial forces.

An analysis indicated that the running-in process of the Si–SiO_x/SiO_2 pair was dominated by removal of the native oxide layer; this may be accompanied by hydrophobization of the contact area on the SiO_2 tip and the silicon surface.

Acknowledgements

The authors are grateful for the financial support from National Basic Research Program (No. 2011CB707604) and Natural Science Foundation of China (51175441, 90923017).

Reference

[1] Bhushan B. Nanotribology and nanomechanics of MEMS/NEMS and BioMEMS/BioNEMS materials and devices. *Microelectro Eng* **84**: 387–412 (2007)

[2] Williams J A, Le H R. Tribology and MEMS. *J Phys D: Appl Phys* **39**: 201–214 (2006)

[3] Kim S H, Asay D B, Dugger M T. Nanotribology and MEMS. *Nano Today* **2**: 22–29 (2007)

[4] Alsem D H, Stach E A, Dugger M T, Enachescu M, Ritchie R O. An electron microscopy study of wear in poly silicon microelectromechanical systems in ambient air. *Thin Solid Films* **515**: 3259–3266 (2007)

[5] Peter J B. *ASM Handbook*. ASM International, 1992.

[6] Nogueira I, Dias A M, Gras R, Progri R. An experimental model for mixed friction during running-in. *Wear* **253**: 541–549 (2002)

[7] Horng J H, Len M L, Lee J S. The contact characteristics of rough surfaces in line contact during running-in process. *Wear* **253**: 899–913 (2002)

[8] Masouros G, Dimarogonas A, Lefas K. A model for wear and surface roughness transients during the running-in of bearings. *Wear* **45**: 375–382 (1977)

[9] Wang X D, Yu J X, Chen L, Qian L M, Zhou Z R. Effects of water and oxygen on the tribochemical wear of monocrystalline Si(100) against SiO_2 sphere by simulating the contact conditions in MEMS. *Wear* **271**: 1681–1688 (2011)

[10] Barnette A L, Asay D B, Kim D, Guyer B D, Lim H, Janik M J, Kim S H. Experimental and density functional theory study of the tribochemical wear behavior of SiO_2 in humid and alcohol vapor environments. *Langmuir* **25**(22): 13052–13061 (2009)

[11] Shen S H, Meng Y G. A novel running-in method for improving life-time of bulk-fabricated silicon MEMS devices. *Tribology Letters* **47**: 273–284 (2012)

[12] Nevshupa R A, Scherge M, Ahmed S I–U. Transitional microfriction behavior of silicon induced by spontaneous water adsorption. *Surf Sci* **517**: 17–28 (2002)

[13] Torii A, Sasaki M, Hane K, Okuma S. A method for determining the spring constant of cantilevers for atomic force microscopy. *Meas Sc. Technol* **7**: 179–184 (1996)

[14] Varenberg M, Etsion I, Halperin G. An improved wedge calibration method for lateral force in atomic force microscopy. *Rev Sci Instrum* **74**: 3362–3367 (2003)

[15] Yu J X, Qian L M, Yu B J, Zhou Z R. Nanofretting behaviors of monocrystalline silicon (100) against diamond tips in atmosphere and vacuum. *Wear* **267**: 322–329 (2009)

[16] Yu J X, Qian L M, Yu B J, Zhou Z R. Nanofretting behavior of monocry stalline Silicon (100) against SiO_2 microsphere in vacuum. *Tribology Letters* **34**: 31–40 (2009)

[17] Fouvry S, Kapsa P, Zahouani H, Vincent L. Wear analysis in fretting of hard coatings through a dissipated energy concept. *Wear* **203-204**: 393–403 (1997)

[18] Tristani L, Zindine E M, Boyer L, Klimek G. Mechanical modeling of fretting cycles in electrical contacts. *Wear* **249**: 12–19 (2001)

[19] Maluf N. An introduction to microelectromechanical systems engineering. *Meas Sci Technol* **13**(2): 229 (2002)

[20] Tambe N, Bhushan B. Friction model for the velocity dependence of nanoscale friction. *Nanotechnology* **16**: 2309–2324 (2005)

[21] Lafaye S, Gauthier C, Schirrer R. The ploughing friction: analytical model with elastic recovery for a conical tip with ablunted spherical extremity. *Tribology Letters* **21**(2): 95–99 (2006)

[22] Bhushan B. *Handbook of Micro/Nanotribology*. Boca Raton, FL.: CRC Press, 1995.

[23] Opitz A, Ahmed S I–U, Schaefer J A, Scherge M. Firiction of thin water films: a nanotribological study. *Surf Sci* **504**: 199–207 (2002)

[24] Vigil G, Xu Z H, Steinberg S, Israelachvili J. Interaction of silica surfaces. *J Colloid Interface Sci* **165**: 367–385 (1994)

[25] Barnette A L, Asay D B, Janik M J, Kim S H. Adsorption isotherm and orientation of alcohols on hydrophilic SiO_2 under ambient conditions. *J Phys Chem C* **113** (24): 10632–10641 (2009)

[26] Mizuhara K, Hsu S M. Tribochemical reaction of oxygen and water on silicon surfaces. *Tribol Ser* **21**: 323–328 (1992)

[27] Xiao X D, Qian L M. Investigation of humidity-dependent capillary force. *Langmuir* **16**: 8153–8158 (2000)

[28] Hsiao E, Marino M J, Kim S H. Effects of gas adsorption isotherm and liquid contact angle on capillary force for sphere-on-flat and cone-on-flat geometries. *J Colloid Interface Sci* **352**(2): 549–557 (2010)

[29] Marino M J, Hsiao E, Chen Y S, Eryilmaz O L, Erdemir A, Kim S H. Understanding run-in behavior of diamond-like carbon friction and preventing diamond-like carbon wear in humid air. *Langmuir* **27**: 12702–12708 (2011)

[30] Katsuki F. Single asperity tribochemical wear of silicon by atomic force microscopy. *J Mater Res* **24**: 173–178 (2009)

[31] Zhu T, Li J, Lin X, Yip S. Stress-dependent molecular pathways of silica-water reaction. *J Mech Phys Solids* **53**: 1597–1623 (2005)

[32] Ioanid A, Dieaconu M, Antohe S. A semiempirical potential model for h-terminated functionalized surface of porous silicon. *Dig J Nanomater Bios* **5**(4): 947–957 (2010)

[33] Goto H, Hirose K, Sakamoto M, Sugiyama K, Inagaki K, Tsuchiya H, Kobata I, Ono T, Mori Y. Chemisorption of OH on the H-terminated Si(001) surface. *Comput Mater Sci* **14**: 77–79 (1999)

[34] Lichtenberger O, Woltersdorf J. On the atomic mechanisms of water-enhanced silicon wafer direct bonding. *Mater Chem Phys* **44**: 222–232 (1996)

[35] Yu J X, Qian L M, Yu B J, Zhou Z R. Effect of surface hydrophilicity on the nanofretting behavior of Si(100) in atmosphere and vacuum. *J Appl Phys* **108**: 034314 (2010)

[36] Yu J X, Kim S H, Yu B J, Qian L M, Zhou Z R. Role of tribochemistry in nanowear of single-crystalline silicon. *ACS Appl Mater Interfaces* **4**(3): 1585–1593 (2012)

Lei Chen. Ph.D candidate in the Tribology Research Institute, Southwest Jiaotong University. His research is focused on the nanowear of silicon and its DLC coating.

Linmao QIAN. Professor of Mechanical Engineering and at Southwest Jiaotong University. He received his BS (1994) and PhD (2000) in mechanical engineering from Tsinghua University in China. After two years at Ecole Normale Supérieure in Paris and one year at the Hong Kong University of Science and Technology as a postdoctoral researcher, he joined the faculty at Southwest Jiaotong University in 2002. His research interest includes nanotribology and nanofabrication. He has published more than 90 peer-reviewed journals papers and authorized 8 patents. He is a member of editorial board of four journals, such as Friction, ISRN Tribology, Frontiers of Mechanical Engineering, and the Proceedings of the Institution of Mechanical Engineers, Part J: Journal of Engineering Tribology. He can be reached at linmao@swjtu.edu.cn.